# Towards a microscopic description of the free-energy landscape of water

Diego Prada-Gracia,[1] Roman Shevchuk,[1] Peter Hamm,[2,a)] and Francesco Rao[1,b)]
[1]*Freiburg Institute for Advanced Studies, School of Soft Matter Research, Freiburg im Breisgau, Germany*
[2]*Institute of Physical Chemistry, University of Zurich, Zurich, Switzerland*

(Received 16 July 2012; accepted 6 September 2012; published online 11 October 2012)

Free-energy landscape theory is often used to describe complex molecular systems. Here, a microscopic description of water structure and dynamics based on configuration-space-networks and molecular dynamics simulations of the TIP4P/2005 model is applied to investigate the free-energy landscape of water. The latter is built on top of a large set of water microstates describing the kinetic stability of local hydrogen-bond arrangements up to the second solvation shell. In temperature space, the landscape displays three different regimes. At around ambient conditions, the free-energy surface is characterized by many short-lived basins of attraction which are structurally well-defined (inhomogeneous regime). At lower temperatures instead, the liquid rapidly becomes homogeneous. In this regime, the free energy is funneled-like, with fully coordinated water arrangements at the bottom of the funnel. Finally, a third regime develops below the temperature of maximal compressibility (Widom line) where the funnel becomes steeper with few interconversions between microstates other than the fully coordinated ones. Our results present a way to manage the complexity of water structure and dynamics, connecting microscopic properties to its ensemble behavior. © *2012 American Institute of Physics*. [http://dx.doi.org/10.1063/1.4755746]

## I. INTRODUCTION

Water is the most studied liquid in nature. Notwithstanding the effort, the debate is still open when it comes to the connection between atomic properties and its ensemble behavior. As an example, the presence of a density maximum at a temperature of 4 °C[1] is qualitatively interpreted as the result of two competing driving forces, i.e., the directionality of hydrogen bonds, favoring tetrahedral (lower-density) water arrangements which are enthalpically stabilized, and entropy maximization by non-directional interactions and disorder, resulting in a closer packing (higher density). Recent experimental and computational evidences pointed out that at ambient conditions these arrangements have distinct structural and dynamical properties.[2–4] These findings might be related to a century-old idea describing water anomalies as an emergent property of a mixture-like liquid.[5–8] This picture is far from conclusive, with other groups providing counter evidences to these proposals.[9–11]

In other fields, a useful approach to clarify the connection between microscopic properties and ensemble behavior makes use of the free-energy paradigm. Energy landscape theory has demonstrated to be a successful approach for the study of the structure and dynamics of complex molecular systems.[12–16] Within this framework, molecular dynamics is interpreted as a trajectory on the multidimensional free-energy surface. The latter is made up of many valleys connected by saddles, suggesting that system dynamics can be divided into intravalley and intervalley motions.[17] The former represent the oscillations around local minima, while the latter involve barrier crossings from one minimum to another.[18]

For the case of water, most descriptions of the energy surface have been limited to ensemble properties or clusters of a few tens of molecules.[19–21] Recently, a mapping of the free-energy surface of bulk water from a more microscopic perspective, an extension of configuration-space-networks,[22,23] was proposed.[3] Network configurations (i.e., nodes) and links represented local water hydrogen-bond arrangements with an extension of two solvation shells and the transitions among them as sampled by molecular dynamics simulations, respectively. This approach represents a reductionist strategy (i.e., focusing on the microscopic properties) to describe the free-energy landscape of water.

In this work, network analysis is extended beyond ambient temperature by running extensive molecular dynamics simulations of the TIP4P/2005 water model from 340 K to the supercooled regime. As the system is cooled down, the free-energy landscape is characterized by three different regimes. At temperatures above the physiological one, the free-energy presents several, short-lived, basins of attraction. Below this temperature, the liquid becomes homogeneous with the development of a funnel-like energy landscape. Finally, by passing the temperature of maximum compressibility the funnel rapidly becomes more pronounced with a very strong bias towards fully coordinated structures.

Within the context of water structure and dynamics, our results provide a framework to link microscopic behavior to water ensemble properties.

## II. METHODS

### A. Molecular dynamics simulations

All molecular dynamics simulations were run with the program GROMACS.[24,25] The water box consisted of 1024

a)phamm@pci.uzh.ch.
b)francesco.rao@frias.uni-freiburg.de.

 © 2012 American Institute of Physics

TIP4P/2005[26] water molecules in the NPT ensemble with pressure of 1 atm and temperatures ranging from 190 K to 340 K with steps of 10 K. The integration time-step was 2 fs, saving coordinates every 4 fs. Equilibration was run for 15 ns, followed by a 2 ns long run to collect the data. For temperatures below 240 K the equilibration time was elongated up to 25 ns. During the production runs, the system was coupled to a Berendsen barostat[27] and a velocity rescale thermostat[28] with coupling times $\tau_P = 1.0$ ps and $\tau_T = 1.0$ ps, respectively. Long range electrostatics was computed with Particle-Mesh-Ewald,[29] using a 1.0 nm cutoff for all non-bonded interactions. Calculations with the TIP3P[30] and TIP5P[31] models were carried out using the same protocol.

### B. Hydrogen bond definitions

The hydrogen bond definition introduced by Skinner and collaborators was used.[32] In this approach the orbital occupancy is parametrized in terms of the intermolecular distance $r$ between the acceptor O and donor H and the angle $\psi$ that the O···H ray makes with the out-of-plane unit vector of the acceptor molecule using the formula:

$$N(r, \psi) = \exp(-r/0.343)(7.1 - 0.050\psi + 0.00021\psi^2). \quad (1)$$

As in the original work, two molecules are considered to be hydrogen-bonded if the occupancy $N(r, \psi)$ exceeds a certain threshold ($N > 0.0085$). To check the robustness of our results with the hydrogen bond definition, the analysis was repeated considering the conventional inter-oxygen distance and angle O–H–O (cutoffs of 3.5 Å and 30°, respectively[33]).

### C. Tetrahedral order parameter

The tetrahedral order parameter for a water molecule $i$ is calculated as

$$q_i = 1 - \frac{3}{8}\sum_{j=1}^{3}\sum_{k=j+1}^{4}\left(\cos\psi_{jik} + \frac{1}{3}\right)^2, \quad (2)$$

where $\psi_{jik}$ is the angle formed by their oxygens.[6] The averaged value of this order parameter over an ensemble of water molecules is denoted as $Q$.

## III. THEORY

Configuration-space-networks (often referred as Markov-State-Models when the Markov property is fulfilled) provide high resolution free-energy landscape representations of complex molecular systems.[18,22,23,34–39] The main idea behind this approach is to map the molecular dynamics onto a transition network where nodes and links represent system configurations and the transitions between them, respectively. System configurations are *microstates*, i.e., very small portions of the accessible configuration space. Within this approach a variety of molecular trajectories from molecular dynamics simulations[18,22,23] to single molecule experiments[40–42] can be analyzed. The great advantage of configuration-space-networks with respect to conventional methods is that free-energy representations are obtained without the use of projections onto arbitrarily chosen order parameters.[22,34] This is in principle equivalent to mapping the underlying potential energy surface into a transition network.[18,43–45]

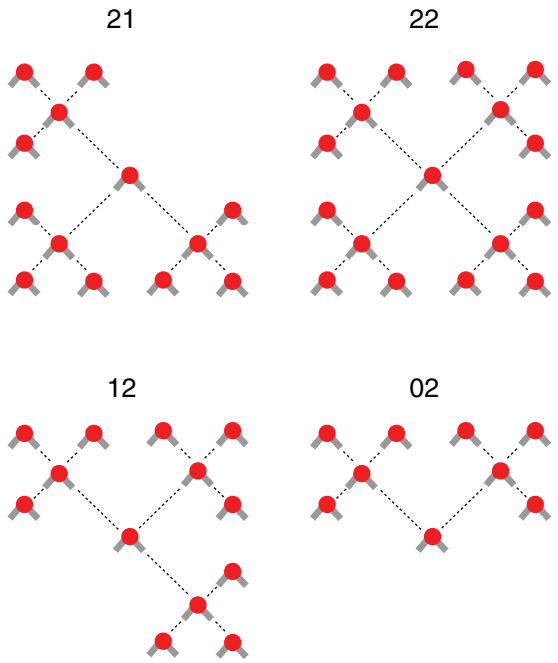


FIG. 1. Representative water microstates belonging to the four most populated gradient-clusters at 300 K. Hydrogen bonds are represented as dashed lines. For simplicity of reference, each of the four configurations is classified by two numbers, indicating the number of donors and acceptors of the central water molecule (e.g., 21 stands for two donors and one acceptor).

Very recently, we showed that configuration-space-networks can be used to map the free-energy landscape of bulk water at ambient conditions.[3] In this case, microstates are defined by hydrogen-bond connectivity patterns including the first and second solvation shells of a given water molecule (see Fig. 1). The characterization of the hydrogen-bond pattern is built in a way that takes into account of the indistinguishable nature of water molecules and all the possible permutations (see Ref. 3 for details). Consequently, the configuration-space-network of water is built by following the evolution of the microstates of each water molecule of the simulation box, resulting in 1024 trajectories of length 2 ns for the present case. Network links are direct molecular transitions between water microstates of the same molecule at a temporal resolution imposed by the saving frequency of Cartesian coordinates (4 fs in the present work). By recording link populations, the final configuration-space-network is equivalent to a transition matrix.

As observed elsewhere,[18,23,34,39] the transition network resulting from this analysis synthetically encodes the complex organization of the underlying free-energy landscape. Specifically, densely connected regions of the network correspond to free-energy basins, i.e., metastable regions of the configuration space. Several algorithms can be used to extract this information, including the max flow theorem,[34] random walks,[23,46] or transition gradient analysis.[39,47] All these approaches aim to clusterize the network into kinetically and structurally well defined basins of attraction.

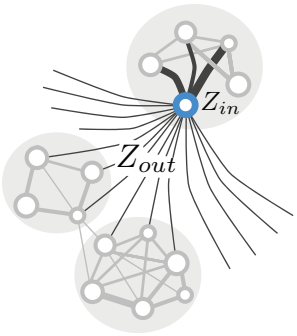


FIG. 2. Configuration-space-networks. Pictorial representation of the relative balance between intra-basin ($Z_{in}$) and inter-basins ($Z_{out}$) transition probabilities from the point of view of a node (in blue). Gray regions represent free-energy basins of attraction as detected by the gradient-algorithm[39,47] (see Sec. III for details).

In enthalpy driven free-energy landscapes, of which proteins are an archetypal example, the transition probability to stay inside a given basin $Z_{in}$ is much larger than the probability to hop outside $Z_{out}$.[18,34] That is, basin hoping is a rare event. Moreover, the number of neighboring basins is usually very limited, with the emergence of well defined transition pathways.[18,22,36] This is not the case for water.[3] Being a liquid, it is mainly characterized by entropic basins of attraction. As illustrated in Fig. 2, $Z_{in}$ and $Z_{out}$ become comparable because the cumulative of the *many* small inter-basin transition probabilities ($Z_{out}$) is similar to the *few* highly populated intra-basin relaxations ($Z_{in}$). In other words, the probability to leave the basin is similar to stay in it. This observation would lead to the conclusion that, at the atomic level, water does not have any type of *configurational* selection. However, this is not true when considering all the contributions to $Z_{out}$ separately:

$$Z_{out} = \sum_i Z_{out}^{(i)}. \tag{3}$$

Structural inhomogeneities, i.e., configurational selection, emerge because

$$\max\left(Z_{in}^{(i)}\right) \gg \max\left(Z_{out}^{(i)}\right), \tag{4}$$

meaning that the probability of an intra-basin transition is larger than hoping to any other *specific* basin. When this condition holds, the environment of a given water molecule alternatively adopts a number of different configurations, each of them characterized by a specific free-energy basin of attraction. This is an emergent property of water at ambient temperature.[3]

Such structural inhomogeneities are found by using a gradient-based approach to cluster the transition network, grouping together water microstates belonging to the same steepest descent free-energy pathway.[3,39,47] From an operative point of view, the algorithm works on a per-node basis by deleting all the links (transitions) but the most visited one (which represents the local direction of the gradient). When applied to the whole network, the algorithm provides a set of disconnected trees, each of them representing a collective pathway of relaxation to the bottom of the *local* free-energy basin of attraction (gradient-cluster, gray regions in Fig. 2). Each gradient-cluster represents a structurally and kinetically well defined molecular arrangement with an extension of up to two solvation shells.[3]

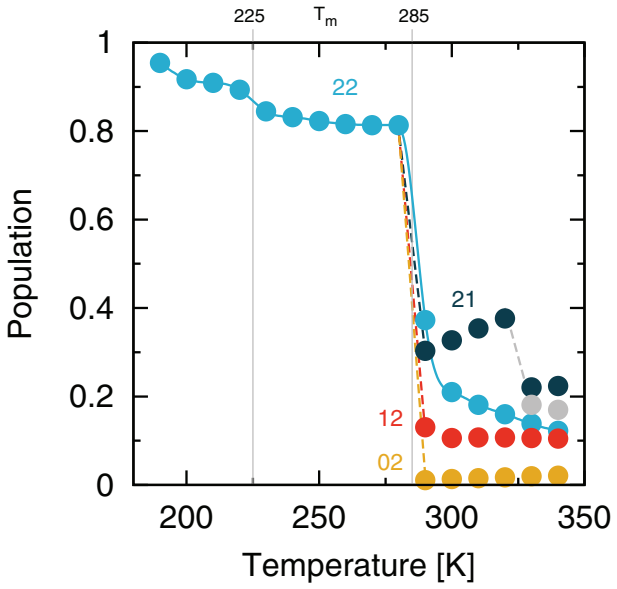


FIG. 3. Population of the most visited gradient-clusters as a function of temperature for the TIP4P/2005 model. Vertical lines correspond to 225 K and 285 K. $T_m$ indicates the melting temperature of the model at around 250 K.[26]

In this contribution, the behavior of these free-energy basins is investigated in temperature space to elucidate the global organization of the free-energy landscape, including the relationship between microscopic behavior and ensemble properties.

## IV. RESULTS AND DISCUSSION

### A. The free-energy landscape of water

Molecular dynamics simulations of the TIP4P/2005 water model at temperatures from 190 K to 340 K were run and their corresponding configuration-space-networks built. For each of these networks, we looked for the free-energy basins characterizing local water arrangements by means of a gradient-cluster analysis (see Sec. III).[3,39,47] In Fig. 3, the population of the most visited gradient-clusters is shown as a function of temperature. At temperatures larger than 285 K, several free-energy basins of attraction were found in agreement with previous analysis on the SPC model at 300 K.[3] The structural configurations at the bottom of the most visited free-energy basins are pictorially represented in Fig. 1. They correspond to the following hydrogen-bond configurations of the central water molecule: 2 donors, 1 acceptor (21, dark blue in Fig. 3, population of 0.32 at 300 K); 2 donors, 2 acceptors (22, light blue, 0.21); 1 donor, 2 acceptors (12, red, 0.13); 0 donors, 2 acceptors (02, yellow, 0.01). At the highest temperatures a fifth basin appears being characterized by a 11 first solvation shell (gray). This acceptor/donor representation is adopted for simplicity but the contribution of the second solvation shell organization is strictly needed when it comes to correctly characterize the free-energy basins (e.g., there are basins of attraction with the same first shell but different second shell[3]).

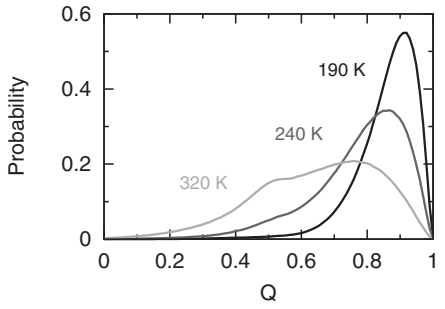


FIG. 4. Distribution of the tetrahedral order parameter $Q$ for the three regimes.

In this temperature range the liquid is *inhomogeneous* in the sense that the local environment of a water molecule interconverts between configurations with distinct structural and dynamical properties. Those represent short-lived metastable arrangements with sub-ps lifetime.[3,4]

Below 285 K this property is lost as shown by the rapid increase of the population of the 22 gradient-cluster to a value larger than 0.8 (light blue in Fig. 3). As such, all highly populated gradient-clusters collapse to 22, being the only largely populated free-energy basin. The population of this basin is almost constant till 225 K. In this regime, the liquid is *homogeneous* and the free-energy landscape resembles a funnel, with the fully coordinated configuration 22 at the bottom of it (see also Sec. II C). The funnel behavior emerges because 22 becomes a global attractor of the dynamics as it is the case for the native state in protein folding.[48] Still, a cumulative population of 0.2 split into roughly six basins survives. These configurations are rich of 4-fold hydrogen-bond loops, slowly interconverting with the fully coordinated configuration.

Below 225 K, i.e., roughly below the temperature of maximum compressibility (estimated to be around 230 K[49]), the entire landscape collapses onto 22 with a much more pronounced funnel behavior (see also Sec. II C). Interestingly, the temperature of maximum compressibility is considered by some as the Widom line, i.e., the propagation of a liquid-liquid critical point located at higher pressure.[8,49,50] If this is so, this water regime would be connected to the mentioned transition. In this temperature region the density assumes its minimum value (see also Fig. 5(d)). For this reason, we refer to this temperature segment as the *low-density* homogeneous regime of the liquid.

It is interesting to compare these regimes with the distribution of the average tetrahedral order parameter $Q$ (see Sec. II).[6] In Fig. 4 data for 320 K, 240 K, and 190 K are shown. At around ambient conditions the distribution is bi-modal (light gray), indicating that the liquid assumes both ordered and disordered atomic arrangements. This property is lost at lower temperatures where the distribution becomes uni-modal (gray) with a small population for values close to 0.5. This sub-population disappears below the temperature of maximum compressibility, resulting in a sharply peaked distribution (dark gray). The shape shift from bi-modal to uni-modal is in good agreement with the change from the inhomogeneous regime to the homogeneous one.

Summarizing this section, three different regimes for the liquid phase of water were found. Each of these regions is characterized by a specific organization of the underlying free-energy landscape as shown by the temperature dependence of the populations of the major free-energy basins (Fig. 3).

### B. Network properties and relation to the density anomaly

As a function of temperature, the number of visited microstates (i.e., nodes) is increasing monotonously, as shown by Fig. 5(a). That is, the higher the temperature the larger

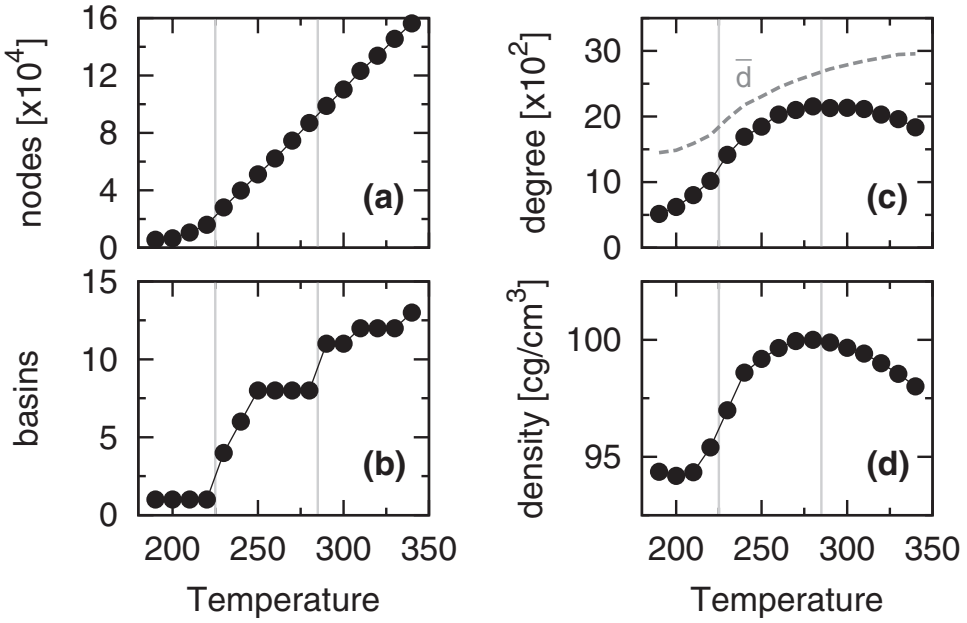


FIG. 5. Topology of the configuration-space-network as a function of temperature. (a) Number of nodes; (b) number of gradient-clusters with a population larger than 0.01; (c) number of connections of the 22 node. For comparison, the average number of connections per node $\bar{d}$ is shown as a dashed line (in this case the multiplicative factor is 1 and not $\times 10^2$); (d) density. Vertical lines correspond to 225 K and 285 K.

the portion of the configuration space visited by the molecular dynamics simulation. Above 225 K the relation is linear but below this temperature the number of microstates changes in a nonlinear way, visiting in proportion a smaller fraction of the configuration space. This behavior might be related to the breakdown of the Einstein diffusion relationship below the temperature of maximum compressibility as observed for the ST2 model.[51]

In Fig. 5(b), the number of gradient-clusters with a population larger than 0.01 as a function of temperature is shown. The data present a step wise behavior, correlating very well with the presence of the three regimes. Interestingly, the number of gradient-clusters is mostly constant in the two low-temperature regimes with only one free-energy basin below 225 K.

From a network topology point of view, the number of connections per node (degree) grows with temperature, going from an average value $\bar{d}$ of 14.5 to 29.5 at 190 K and 340 K, respectively (dashed line in Fig. 5(c)). This is not the case for the node degree of the microstate 22. As shown in Fig. 5(c), the degree increases up to around 285 K. Then it starts to decrease where the liquid changes from the homogeneous regime to the inhomogeneous one.

Comparison with density (Fig. 5(d)) shows a remarkable correlation. With a Pearson coefficient of 0.98, the behavior of the node degree of microstate 22 correlates with the density anomaly. This seems an interesting fact connecting an ensemble property like the density to a purely microscopic quantity, i.e., the number of accessible transitions from the fully coordinated configuration 22.

### C. The origin of a funneled energy landscape

In this section, characteristic properties of the transition network corresponding to the three regimes are illustrated. In the higher temperatures regime, structural inhomogeneities emerge because the maximum of the transition probability $\max(Z^{(i)})$ points towards the attractor of the basin (e.g., $\tilde{Z}$ in the pictorial representation of Fig. 6(a)). This is not the case below 285 K where the transition to 22 ($Z_{22}$) becomes the maximum of the transition probability for many nodes which were acting as attractors at higher temperatures.

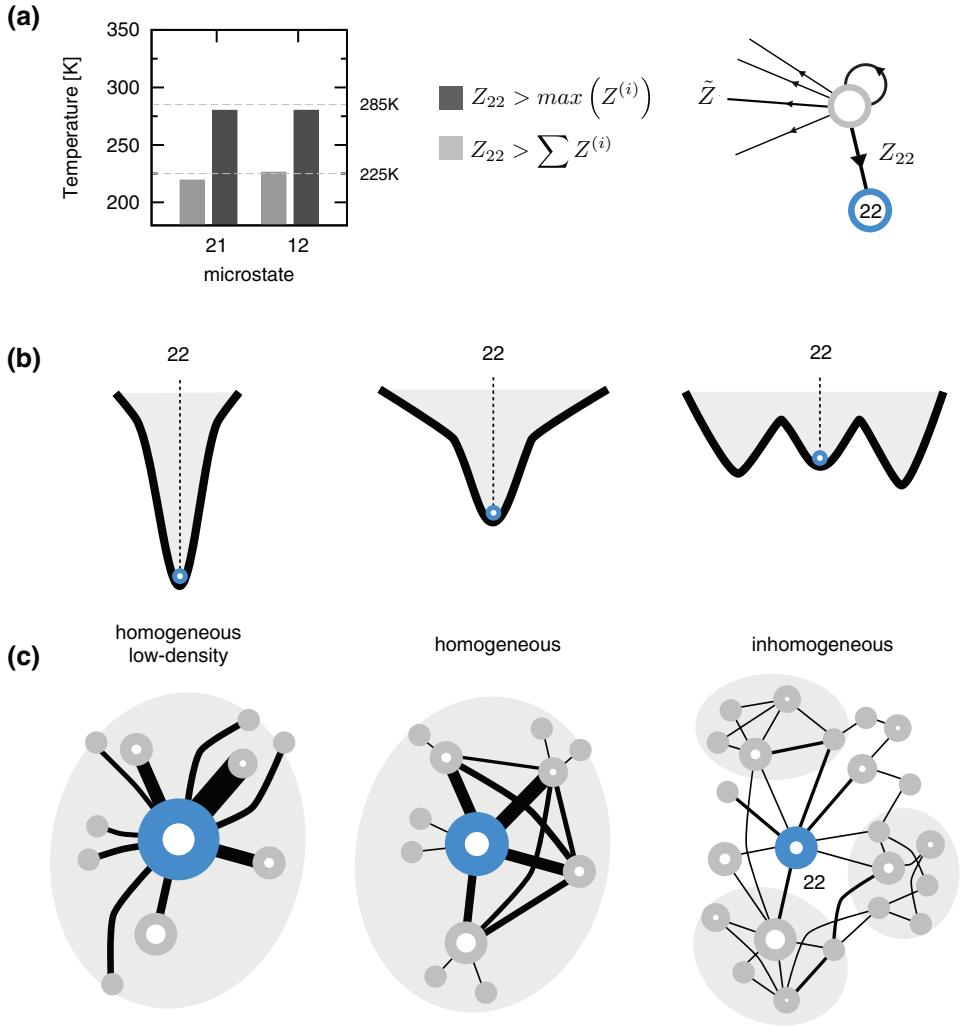


FIG. 6. Schematic representations of the three regimes of liquid water; (a) temperatures at which there is a change in the transition probability maximum for the 21 and 12 microstates (see Sec. IV for details); (b) free-energy landscape representation; (c) network representation.

Figure 6(a) shows the temperature at which $Z_{22} = \max(Z^{(i)})$ for the relevant microstates 21 and 12 (dark gray bars). Relaxing directly to 22, they do not build basins of attraction anymore. For nodes not directly connected to 22 the relaxation process to it goes through two or more steps like for 02. Consequently, a free-energy landscape characterized by a single predominant minimum (22) develops. This type of landscapes recalls the well-known funnel-landscape paradigm applied to protein folding.[48,52,53]

Below 225 K, $Z_{22}$ drives the dynamics in a even stronger way being the corresponding transition larger than the cumulative of all other transitions, i.e., $Z_{22} > \sum_i Z^{(i)}$ (gray bars in Fig. 6(a)). In other words, every time a water molecule assumes a configuration different from 22, the probability to go back to 22 is larger with respect to the cumulative of any other transition.

From a qualitative point of view the three regimes of the free-energy landscape are represented in Fig. 6(b) (in panel c a pictorial representation of the underlying network).

### D. Robustness and limitations of the current methodology

Other water models show the same three regimes as TIP4P/2005. In Fig. 7(a), the population of the most visited gradient-clusters for the TIP3P and TIP5P models is shown. The two models are in qualitative agreement with the analysis done for TIP4P/2005 where the exact temperature values characterizing the three regimes depend on the specific water model used. This is expected due to the recently observed model dependent temperature shifts.[54] That is, while hydrogen-bond patterns between different water models are essentially the same, they differ by a temperature shift of up to ∼65 K for the TIP3P model when comparing conventional

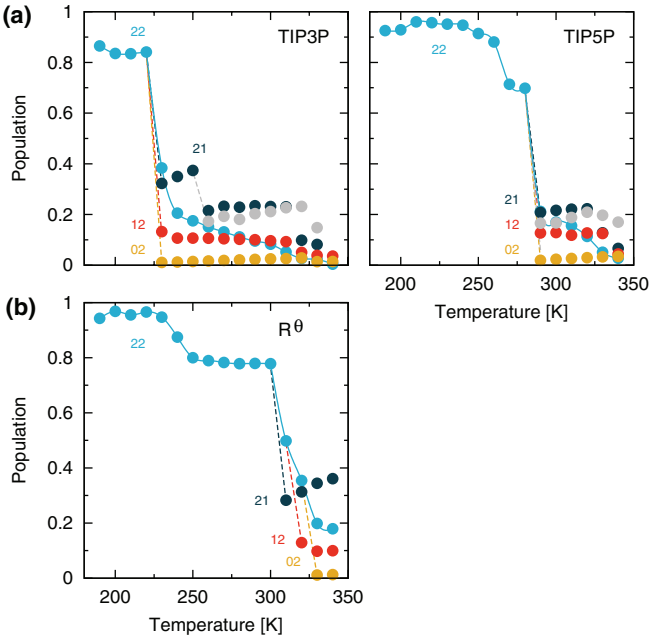


FIG. 7. Robustness of the gradient-cluster analysis. (a) Gradient-cluster populations for TIP3P and TIP5P water models and (b) for TIP4P/2005 by using the $R\theta$ hydrogen-bond definition.

classical water models to TIP4P/2005. For example, the appearance of the homogeneous regime is found at 225 K for TIP3P, at a roughly 60 K lower temperature than TIP4P/2005 in excellent agreement with previous analysis.[54] Similarly, the case of TIP5P is in qualitative agreement with TIP4P/2005.

The origin of the temperature shift is related to the relative hydrogen-bond strength of the various models.[54] Consequently, it is expected that artificial modifications of the hydrogen-bond strength due to more (or less) conservative bond definitions might shift the three regimes as well. This is so because water microstates are based on hydrogen-bond connectivity and its propensity. To check this behavior, the whole analysis was repeated by using another definition of hydrogen-bond based on the classical inter-oxygen distance and donor-acceptor angle $R\theta$ (see Sec. II). As shown in Fig. 7(b), the overall behavior of the gradient-cluster populations is remarkably similar with the presence of the three liquid regimes. On the other hand, the expected temperature shift is present. We found that $R\theta$ predicts a larger number of hydrogen bonds than the Skinner definition. For the former definition, 3.8 and 3.6 average number of hydrogen bonds per molecule were found at temperatures of 250 K and 300 K, respectively. These numbers decreased to 3.7 and 3.3 when the Skinner definition was used. Using a less conservative definition like $R\theta$, effectively increases hydrogen-bond strength. As a consequence, the population of the fully coordinated gradient-cluster is over estimated, giving in turn a temperature shift. Since the discussion on the quality of hydrogen-bond definitions is still open,[32,55] we want to remark that the change of the hydrogen-bond definition would only slightly affect the exact position of the three regimes but not the existence of them.

## V. CONCLUSIONS

We have presented extensive molecular dynamics simulations of the TIP4P/2005 model for a temperature interval ranging from 190 K to 340 K in conjunction with complex network analysis to obtain a detailed mapping of the underlying free-energy landscape. The main idea was to investigate the structural and dynamical properties of local water configurations defined by the hydrogen-bond connectivity with an extension of two solvation shells.

From a microscopic point of view, the free-energy landscape of liquid water is characterized by three major regimes. At ambient conditions, several metastable water configurations with distinct structure and dynamics are found (*inhomogeneous* regime). Below 285 K, the free-energy landscape develops a funnel dominated by the fully coordinated configuration with an extension of at least two solvation shells (*homogeneous* regime). By lowering the temperature below 225 K, the funnel becomes more pronounced, with the fully coordinated configuration becoming a global attractor of the dynamics (homogeneous *low-density* regime).

While the three regimes were deducted from water microscopic properties, the presence of the tree regimes is correlated to the behavior of the density curve, which is an ensemble property of the system. As such, the homogeneous low-density regime spans till the density starts to grow with

a change in concavity at 225 K; the homogeneous regime is characterized by the monotonous increase of the density curve up to the density maximum at around 280 K; finally, the descending section of the density is located into the inhomogeneous regime.

From an experimental point of view, the presence of structural inhomogeneities at ambient temperature is in qualitative agreement with small-angle x-ray scattering measurements[2] while the presence of multiple kinetics is in principle accessible to high order nonlinear spectroscopy.[4]

## ACKNOWLEDGMENTS

This work is supported by the Excellence Initiative of the German Federal and State Governments (F.R.) and by the Swiss National Science Foundation (SNF) through the NCCR MUST (P.H.).

[1]R. Waller, *Essayes of Natural Experiments. Secretary of the Academie del Cimento (1684)* (reprinted by Johnson Reprint Corporation, New York, 1964).
[2]C. Huang, K. T. Wikfeldt, T. Tokushima, D. Nordlund, Y. Harada, U. Bergmann, M. Niebuhr, T. M. Weiss, Y. Horikawa, M. Leetmaa, M. P. Ljungberg, O. Takahashi, A. Lenz, L. Ojamäe, A. P. Lyubartsev, S. Shin, L. G. M. Pettersson, and A. Nilsson, Proc. Natl. Acad. Sci. U.S.A. **106**, 15214 (2009).
[3]F. Rao, S. Garrett-Roe, and P. Hamm, J. Phys. Chem. B **114**, 15598 (2010).
[4]S. Garrett-Roe, F. Perakis, F. Rao, and P. Hamm, J. Phys. Chem. B **115**, 6976 (2011).
[5]W. C. Röntgen, Ann. Phys. **281**, 91 (1892).
[6]J. R. Errington and P. G. Debenedetti, Nature (London) **409**, 318 (2001).
[7]M. J. Cuthbertson and P. H. Poole, Phys. Rev. Lett. **106**, 115706 (2011).
[8]K. T. Wikfeldt, C. Huang, A. Nilsson, and L. G. M. Pettersson, J. Chem. Phys. **134**, 214506 (2011).
[9]G. N. I. Clark, G. L. Hura, J. Teixeira, A. K. Soper, and T. Head-Gordon, Proc. Natl. Acad. Sci. U.S.A. **107**, 14003 (2010).
[10]E. B. Moore and V. Molinero, Nature (London) **479**, 506 (2011).
[11]D. T. Limmer and D. Chandler, J. Chem. Phys. **135**, 134503 (2011).
[12]M. Goldstein, J. Chem. Phys. **51**, 3728 (1969).
[13]F. H. Stillinger, Science **267**, 1935 (1995).
[14]P. G. Wolynes, J. N. Onuchic, and D. Thirumalai, Science **267**, 1619 (1995).
[15]J. N. Onuchic, Z. Luthey-Schulten, and P. G. Wolynes, Annu. Rev. Phys. Chem. **48**, 545 (1997).
[16]D. J. Wales, M. A. Miller, and T. R. Walsh, Nature (London) **394**, 758 (1998).
[17]H. Frauenfelder, S. G. Sligar, and P. G. Wolynes, Science **254**, 1598 (1991).
[18]F. Rao and M. Karplus, Proc. Natl. Acad. Sci. U.S.A. **107**, 9152 (2010).
[19]C. A. Angell, Science **267**, 1924 (1995).
[20]D. J. Wales and M. P. Hodges, Chem. Phys. Lett. **286**, 65 (1998).
[21]R. Ludwig, Angew. Chem. Int. Edit. **40**, 1808 (2001).
[22]F. Rao and A. Caflisch, J. Mol. Biol. **342**, 299 (2004).
[23]D. Gfeller, P. De Los Rios, A. Caflisch, and F. Rao, Proc. Natl. Acad. Sci. U.S.A. **104**, 1817 (2007).
[24]D. Van Der Spoel, E. Lindahl, B. Hess, G. Groenhof, A. E. Mark, and H. J. C. Berendsen, J. Comput. Chem. **26**, 1701 (2005).
[25]B. Hess, C. Kutzner, D. van der Spoel, and E. Lindahl, J. Chem. Theory Comput. **4**, 435 (2008).
[26]J. L. F. Abascal and C. Vega, J. Chem. Phys. **123**, 234505 (2005).
[27]H. J. C. Berendsen, J. P. M. Postma, W. F. van Gunsteren, A. DiNola, and J. R. Haak, J. Chem. Phys. **81**, 3684 (1984).
[28]G. Bussi, D. Donadio, and M. Parrinello, J. Chem. Phys. **126**, 014101 (2007).
[29]T. Darden, D. York, and L. Pedersen, J. Chem. Phys. **98**, 10089 (1993).
[30]W. L. Jorgensen, J. Chandrasekhar, J. D. Madura, R. W. Impey, and M. L. Klein, J. Chem. Phys. **79**, 926 (1983).
[31]M. W. Mahoney and W. L. Jorgensen, J. Chem. Phys. **112**, 8910 (2000).
[32]R. Kumar, J. R. Schmidt, and J. L. Skinner, J. Chem. Phys. **126**, 204107 (2007).
[33]A. Luzar and D. Chandler, Phys. Rev. Lett. **76**, 928 (1996).
[34]S. V. Krivov and M. Karplus, Proc. Natl. Acad. Sci. U.S.A. **101**, 14766 (2004).
[35]D. Gfeller, D. M. de Lachapelle, P. De Los Rios, G. Caldarelli, and F. Rao, Phys. Rev. E **76**, 026113 (2007).
[36]F. Noé, I. Horenko, C. Schütte, and J. C. Smith, J. Chem. Phys. **126**, 155102 (2007).
[37]J. D. Chodera, N. Singhal, V. S. Pande, K. A. Dill, and W. C. Swope, J. Chem. Phys. **126**, 155101 (2007).
[38]F. Noé and S. Fischer, Curr. Opin. Struct. Biol. **18**, 154 (2008).
[39]D. Prada-Gracia, J. Gómez-Gardeñes, P. Echenique, and F. Falo, PLoS Comput. Biol. **5**, e1000415 (2009).
[40]A. Baba and T. Komatsuzaki, Proc. Natl. Acad. Sci. U.S.A. **104**, 19297 (2007).
[41]P. Schuetz, R. Wuttke, B. Schuler, and A. Caflisch, J. Phys. Chem. B **114**, 15227 (2010).
[42]A. Baba and T. Komatsuzaki, *Single-Molecule Biophysics* (John Wiley & Sons, Inc., 2011), p. 299.
[43]R. E. Kunz and R. S. Berry, J. Chem. Phys. **103**, 1904 (1995).
[44]D. J. Wales, Int. Rev. Phys. Chem. **25**, 237 (2006).
[45]B. Strodel and D. J. Wales, Chem. Phys. Lett. **466**, 105 (2008).
[46]S. van Dongen, "Graph clustering by flow simulation," Ph.D. dissertation (University of Utrecht, The Netherlands, 2000).
[47]F. Rao, J. Phys. Chem. Lett. **1**, 1580 (2010).
[48]K. A. Dill and H. S. Chan, Nat. Struct. Biol. **4**, 10 (1997).
[49]J. L. F. Abascal and C. Vega, J. Chem. Phys. **133**, 234502 (2010).
[50]O. Mishima and H. E. Stanley, Nature (London) **396**, 329 (1998).
[51]P. Kumar, S. V. Buldyrev, S. R. Becker, P. H. Poole, F. W. Starr, and H. E. Stanley, Proc. Natl. Acad. Sci. U.S.A. **104**, 9575 (2007).
[52]P. E. Leopold, M. Montal, and J. N. Onuchic, Proc. Natl. Acad. Sci. U.S.A. **89**, 8721 (1992).
[53]J. D. Bryngelson, J. N. Onuchic, N. D. Socci, and P. G. Wolynes, Proteins **21**, 167 (1995).
[54]R. Shevchuk, D. Prada-Gracia, and F. Rao, J. Phys. Chem. B **116**, 7538 (2012).
[55]R. H. Henchman and S. J. Irudayam, J. Phys. Chem. B **114**, 16792 (2010).